# Sum-Rule Conserving Spectral Functions from the Numerical Renormalization Group

Andreas Weichselbaum and Jan von Delft

*Physics Department, Arnold Sommerfeld Center for Theoretical Physics, and Center for NanoScience,*
*Ludwig-Maximilians-Universität München, D-80333 München, Germany*

We show how spectral functions for quantum impurity models can be calculated very accurately using a complete set of discarded numerical renormalization group eigenstates, recently introduced by Anders and Schiller. The only approximation is to judiciously exploit energy scale separation. Our derivation avoids both the overcounting ambiguities and the single-shell approximation for the equilibrium density matrix prevalent in current methods, ensuring that relevant sum rules hold rigorously and spectral features at energies below the temperature can be described accurately.

Quantum impurity models describe a quantum system with a small number of discrete states, the "impurity," coupled to a continuous bath of fermionic or bosonic excitations. Such models are relevant for describing transport through quantum dots, for the treatment of correlated lattice models using dynamical mean field theory, or for the modeling of the decoherence of qubits.

The impurity's dynamics in thermal equilibrium can be characterized by spectral functions of the type $\mathcal{A}^{\mathcal{BC}}(\omega) = \int \frac{dt}{2\pi} e^{i\omega t} \langle \hat{\mathcal{B}}(t)\hat{\mathcal{C}} \rangle_T$. Their Lehmann representation reads

$$\mathcal{A}^{\mathcal{BC}}(\omega) = \sum_{a,b} \langle b|\hat{\mathcal{C}}|a\rangle \frac{e^{-\beta E_a}}{Z} \langle a|\hat{\mathcal{B}}|b\rangle \delta(\omega - E_{ba}), \quad (1)$$

with $Z = \sum_a e^{-\beta E_a}$ and $E_{ba} = E_b - E_a$, which implies the sum rule $\int d\omega \mathcal{A}^{\mathcal{BC}}(\omega) = \langle \hat{\mathcal{B}}\hat{\mathcal{C}} \rangle_T$. In this Letter, we describe a strategy for numerically calculating $\mathcal{A}^{\mathcal{BC}}(\omega)$ that, in contrast to previous methods, rigorously satisfies this sum rule and accurately describes both high *and* low frequencies, including $\omega \lesssim T$, which we test by checking our results against exact Fermi-liquid relations.

Our work builds on Wilson's numerical renormalization group (NRG) method [1]. Wilson discretized the environmental spectrum on a logarithmic grid of energies $\Lambda^{-n}$ (with $\Lambda > 1$, $1 \leq n \leq N \to \infty$), with exponentially high resolution of low-energy excitations, and mapped the impurity model onto a "Wilson tight-binding chain," with hopping matrix elements that decrease exponentially as $\Lambda^{-n/2}$ with site index $n$. Because of this separation of energy scales, the Hamiltonian can be diagonalized iteratively: adding one site at a time, a new "shell" of eigenstates is constructed from the new site's states and the $M_K$ lowest-lying eigenstates of the previous shell (the so-called "kept" states), while "discarding" the rest.

Subsequent authors [2–10] have shown that spectral functions such as $\mathcal{A}^{\mathcal{BC}}(\omega)$ can be calculated via the Lehmann sum, using NRG states (kept and discarded) of those shells $n$ for which $\omega \sim \Lambda^{-n/2}$. Though plausible on heuristic grounds, this strategy entails double-counting

ambiguities [5] about how to combine data from successive shells. Patching schemes [9] for addressing such ambiguities involve arbitrariness. As a result, the relevant sum rule is not satisfied rigorously, with typical errors of a few percent. Also, the thermal density matrix (DM) $\hat{\rho} = e^{-\beta \hat{H}}/Z$ has until now been represented rather crudely using only the single $N_T$th shell for which $T \simeq \Lambda^{-1/2(N_T-1)}$ [8], with a chain of length $N = N_T$, resulting in inaccurate spectral information for $\omega \lesssim T$. In this Letter we avoid these problems by using in the Lehmann sum an approximate but *complete* set of eigenstates, introduced recently by Anders and Schiller (AS) [11].

*Wilson's truncation scheme.*—The Wilson chain's zeroth site represents the bare impurity Hamiltonian $\hat{h}_0$ with a set of $d_0$ impurity states $|\sigma_0\rangle$. It is coupled to a fermionic chain, whose $n$th site ($1 \leq n \leq N$) represents a set of $d$ states $|\sigma_n\rangle$, responsible for providing energy resolution to the spectrum at scale $\Lambda^{-n/2}$. For a spinful fermionic band, for example, $\sigma_n \in \{0, \uparrow, \downarrow, \uparrow\downarrow\}$, hence $d = 4$. (Bosonic chains can be treated similarly [10].) The Hamiltonian $\hat{H} = \hat{H}_N$ for the full chain is constructed iteratively by adding one site at a time, using $\hat{H}_n = \hat{H}_{n-1} + \hat{h}_n$ (acting in a $d^n d_0$-dimensional Fock space $\mathcal{F}_n$ spanned by the basis states $\{|\sigma_n\rangle \otimes \cdots \otimes |\sigma_0\rangle\}$), where $\hat{h}_n$ links sites $n$ and $n-1$ with hopping strength $\sim \Lambda^{-n/2}$. Since the number of eigenstates of $\hat{H}_n$ grows exponentially with $n$, Wilson proposed the following iterative truncation scheme to numerically diagonalize the Hamiltonian: Let $n_0$ be the last iteration for which a complete set $\{|s\rangle_{n_0}^K\}$ of kept eigenstates of $\hat{H}_{n_0}$ can be calculated without trunction. For $n > n_0$, construct the orthonormal eigenstates $\{|s\rangle_n^X\}$ of $\hat{H}_n$ (the $n$th "shell"), with eigenvalues $E_s^n$, as linear combinations of the kept eigenstates $|s\rangle_{n-1}^K$ of $\hat{H}_{n-1}$ and the states $|\sigma_n\rangle$ of site $n$,

$$|s'\rangle_n^X = \sum_{\sigma_n s}^K |\sigma_n\rangle \otimes |s\rangle_{n-1}^K [A_{KX}^{[\sigma_n]}]_{ss'}, \quad (2)$$

with coefficients arranged into a matrix $A_{KX}^{[\sigma_n]}$ whose ele-

ments are labeled by $ss'$. The superscript $X = K$ or $D$ indicates that the new shell has been partitioned into "kept" states (say the $M_K$ lowest-lying eigenstates of $\hat{H}_n$) to be retained for the next iteration and "discarded" states (the remaining ones). Since $\hat{h}_n$ acts as a weak perturbation (of relative size $\Lambda^{-1/2}$) on $\hat{H}_{n-1}$, the $d$-fold degeneracy of the states $|\sigma_n\rangle \otimes |s\rangle_{n-1}^X$ is lifted, resulting in a characteristic energy spacing $\Lambda^{-n/2}$ for shell $n$. Iterating until the spectrum of low-lying eigenvalues has reached a fixed point (for $n = N$, say), one generates a set of eigenstates $\{|s\rangle_n^X\}$ with the structure of matrix product states [12] (Fig. 1). The states generated for the last $N$th shell will all be regarded as discarded [11].

*Anders-Schiller basis.*—Recently, AS have shown [11] that the discarded states can be used to build a complete basis for the whole Wilson chain: the states $\{|s\rangle_n^X\}$ describing the $n$th shell are supplemented by a set of $d^{N-n}$ degenerate "environmental" states $\{|e_n\rangle = |\sigma_N\rangle \otimes \cdots \otimes |\sigma_{n+1}\rangle\}$ spanning the rest of the chain to construct the set of states $\{|se\rangle_n^X \equiv |e_n\rangle \otimes |s\rangle_n^X\}$. These reside in the complete Fock space $\mathcal{F}_N$ of the full chain, spanning $\mathcal{F}_N$ if $n \leq n_0$. Ignoring the degeneracy-lifting effect of the rest of the chain, these states become approximate eigenstates of the Hamiltonian $\hat{H}_N$ of the *full* chain ("NRG approximation"),

$$\hat{H}_N |se\rangle_n^X \simeq E_s^n |se\rangle_n^X, \qquad (3)$$

with eigenenergies *independent* of the $(d^{N-n})$-fold degenerate environmental index $e_n$. (This will facilitate tracing out the environment below.) By construction, we have $_m^D\langle se|s'e'\rangle_n^D = \delta_{mn}\delta_{e_n e_n'}\delta_{ss'}$ and

$$_m^K\langle se|s'e'\rangle_n^D = \begin{cases} 0, & m \geq n \\ \delta_{e_n e_n'}[A_{KK}^{\sigma_{m+1}} \ldots A_{KD}^{\sigma_n}]_{ss'}, & m < n. \end{cases} \quad (4)$$

The discarded states of shell $n$ are orthogonal to the discarded states of any other shell, and to the kept states of that or any later shell. Combining the discarded states from all shells thus yields a complete set of NRG eigenstates of $\hat{H}_N$, the "Anders-Schiller basis," that span the full Fock space $\mathcal{F}_N$ ($\sum_n$ henceforth stands for $\sum_{n>n_0}^N$):

$$\mathbf{1}^{(d_0 d^N)} = \sum_{se} |se\rangle_{n_0}^K {}_{n_0}^K\langle se| = \sum_n \sum_{se} |se\rangle_n^{DD} {}_n^{\phantom{D}}\langle se|. \quad (5)$$

*Local operators.*—Let us now consider a "local" operator $\hat{\mathcal{B}}$ acting nontrivially only on sites up to $n_0$. Two
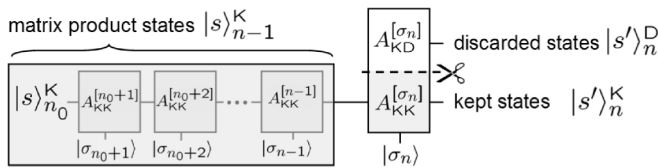


FIG. 1. Diagram for the kept (or discarded) matrix product state $|s'\rangle_n^K$ (or $|s'\rangle_n^D$): the $n$th box represents the matrix block $A_{KX}^{[\sigma_n]}$, its left, bottom, and right legs carry the labels of the states $|s\rangle_{n-1}^K$, $|\sigma_n\rangle$, and $|s'\rangle_n^K$ (or $|s'\rangle_n^D$), respectively.

particularly useful representations are

$$\hat{\mathcal{B}} = \sum_{ss'e} |se\rangle_{n_0}^K [\mathcal{B}_{KK}^{[n_0]}]_{ss'}{}_{n_0}^K\langle s'e| = \sum_n \sum_{XX'}^{\neq KK} \hat{\mathcal{B}}_{XX'}^{[n]}. \quad (6)$$

The left equality, written $\hat{\mathcal{B}} = \hat{\mathcal{B}}_{KK}^{[n_0]}$ in brief, represents the operator in the complete basis set $\{|se\rangle_{n_0}^K\}$, with matrix elements known exactly numerically (possibly up to fermionic minus signs depending on the environmental states, but these enter quadratically in correlation functions and hence cancel). The right-hand side (RHS) of Eq. (6) expresses $\hat{\mathcal{B}}$ in the AS basis and is obtained as follows: starting from $\hat{\mathcal{B}}_{KK}^{[n_0]}$, one iteratively refines the "kept-kept" part of $\hat{\mathcal{B}}$ from, say, the $(n-1)$th iteration in terms of the NRG eigenstates $\{|se\rangle_n^x\}$ of the next shell, including both kept and discarded states ($X = K, D$),

$$\hat{\mathcal{B}}_{KK}^{[n-1]} = \sum_{XX'}\sum_{ss'e} |se\rangle_n^X [\mathcal{B}_{XX'}^{[n]}]_{ss'}{}_n^{X'}\langle s'e| = \sum_{XX'} \hat{\mathcal{B}}_{XX'}^{[n]}, \quad (7)$$

thereby defining the operators $\hat{\mathcal{B}}_{XX'}^{[n]}$, with matrix elements $[\mathcal{B}_{XX'}^{[n]}]_{ss'} = [A_{XK}^{[\sigma_n]\dagger}\mathcal{B}_{KK}^{[n-1]}A_{KX'}^{[\sigma_n]}]_{ss'}$. Splitting off all $XX' \neq KK$ terms ($DD$, $KD$, $DK$) and iteratively refining each $KK$ term until $n = N$, we obtain the RHS of Eq. (6). It has two important features. First, the matrix elements of the time-dependent operator $\hat{\mathcal{B}}(t) = e^{i\hat{H}t}\hat{\mathcal{B}}e^{-i\hat{H}t}$, evaluated within the NRG approximation, $[\mathcal{B}_n^{XX'}(t)]_{ss'} \simeq [\mathcal{B}_n^{XX'}]_{ss'}e^{it(E_s^n - E_{s'}^n)}$, contain differences of eigenenergies from the *same* shell only, i.e., calculated with the same level of accuracy. Second, by *excluding KK* terms it rigorously avoids the double-counting ambiguities and heuristic patching rules plaguing previous approaches [2–10].

*Thermal averages.*—To calculate thermal averages $\langle \ldots \rangle_T = \text{Tr}[\hat{\rho} \ldots]$, we write the full density matrix (FDM) $\hat{\rho} = e^{-\beta\hat{H}}/Z$ using the NRG approximation Eq. (3),

$$\hat{\rho} \simeq \sum_n \sum_{se} |se\rangle_n^D \frac{e^{-\beta E_s^n}}{Z} {}_n^D\langle se| = \sum_n w_n \hat{\rho}_{DD}^{[n]}, \quad (8)$$

where $w_n \equiv d^{N-n}Z_n^D/Z$ and $Z_n^D \equiv \sum_s^D e^{-\beta E_s^n}$. The RHS of Eq. (8) expresses $\hat{\rho}$ as sum over $\hat{\rho}_{DD}^{[n]}$, the density matrix for the *discarded* states of shell $n$, properly normalized as $\text{Tr}[\hat{\rho}_{DD}^{[n]}] = 1$, and entering with relative weight $w_n$, with $\sum_n w_n = 1$. Similarly, for spectral functions we have

$$\langle \ldots \rangle_T = \sum_n w_n \langle \ldots \rangle_n, \quad \mathcal{A}(\omega) = \sum_n w_n \mathcal{A}_n(\omega), \quad (9)$$

where the averages $\langle \cdots \rangle_n$ and spectral functions $\mathcal{A}_n(\omega)$ are calculated with respect to $\hat{\rho}_{DD}^{[n]}$ of shell $n$ only.

Previous strategies [4–11] for thermal averaging amount to using a "single-shell approximation" $w_n = \delta_{nN_T}$ for the density matrix and terminating the chain at a length $N = N_T$ set by $T \simeq \Lambda^{-1/2(N_T-1)}$. As a result, spectral features on scales $\omega \leq T$, which would require a longer chain, are described less accurately [see Figs. 2(a) and 2(b)]. Our

novel approach avoids these problems by using the *full* density matrix (FDM), summed over *all* shells, letting the weighting function $w_n$ select the shells relevant for a given temperature yielding a smooth $T$ dependence [see Fig. 2(c)]. Since $w_n$ has a peak width of five to ten shells depending on $\Lambda$, $d$ and $M_K$ and peaks at $n$ values somewhat above $N_T$ [arrow Fig. 2(b)], spectral information from energies well below $T$ is retained.

Let us now consider the spectral function $\mathcal{A}^{\mathcal{BC}}(\omega)$, for local operators $\hat{B}$ and $\hat{C}$. Equations (4), (6), (8), and (9) can be used to evaluate $\langle \hat{B}(t)\hat{C}\rangle_n$. Fourier transforming the result we find (sums over $ss'$ and $\sigma_n$ implied)

$$\mathcal{A}_n^{\mathcal{BC}}(\omega) = \sum_{m>n_0}^{n} \sum_{XX'}^{\neq KK} [\mathcal{C}_{X'X}^{[m]}\rho_{XX}^{[mn]}]_{s's} [\mathcal{B}_{XX'}^{[m]}]_{ss'}\delta(\omega - E_{s's}^m),$$

$$[\rho_{DD}^{[m=n]}]_{ss'} = \delta_{ss'}\frac{e^{-\beta E_s^n}}{Z_n}, \qquad (10)$$

$$[\rho_{KK}^{[m<n]}]_{ss'} = [A_{KK}^{[\sigma_{m+1}]}\ldots A_{KD}^{[\sigma_n]}\rho_{DD}^{[nn]}A_{DK}^{[\sigma_n]\dagger}\ldots A_{KK}^{[\sigma_{m+1}]\dagger}]_{ss'}.$$

Similarly, the static quantity $\langle \hat{B}\hat{C}\rangle_n$ equals the first line's RHS without the $\delta$ function. The matrix elements $[\rho_{XX}^{[mn]}]_{ss'} \equiv \sum_{em}^{X}\langle se|\hat{\rho}_{DD}^{[n]}|s'e\rangle_m^X$ are given by the second and third lines, together with $\rho_{KK}^{[m=n]} = \rho_{DD}^{[m<n]} = 0$. After performing a "forward run" to generate all relevant NRG eigenenergies and matrix elements, $\mathcal{A}^{\mathcal{BC}}(\omega)$ can be calculated in a single "backward run," performing a sum with the structure $\sum_{m>n_0}^{N}[\mathcal{C}\rho^{\text{red}}\mathcal{B}\cdot\delta()]^{[m]}$, starting from $m = N$. Here $\rho_{XX}^{[m],\text{red}} \equiv \sum_{n\geq m}^{N}w_n\rho_{XX}^{[mn]}$ (updated one site at a time during the backward run) is the *full* reduced density matrix for shell $m$, obtained iteratively by tracing out all shells at smaller scales $\Lambda^{-n/2}$ ($n \geq m$).

Equations (8)–(10) are the main results of our "FDM-NRG" approach. They rigorously generalize Hofstetter's DM-NRG [8] (which leads to similar expressions, but using $w_n = \delta_{nN_T}$ and without excluding $KK$ matrix elements), and provide a concise prescription, free from double-counting ambiguities, for how to combine NRG data from different shells when calculating $\mathcal{A}^{\mathcal{BC}}(\omega)$. The relevant sum rule is satisfied *identically*, since by construction $\int d\omega \mathcal{A}_n^{\mathcal{BC}}(\omega) = \langle \hat{B}\hat{C}\rangle_n$ holds for every $n$ and arbitrary temperature and NRG parameters $\Lambda$ and $M_K$.

*Smoothing discrete data.*—We obtain smooth curves for $\mathcal{A}^{\mathcal{BC}}(\omega)$ by broadening the discrete $\delta$ functions in Eq. (10) using a broadening kernel that smoothly interpolates from a log-Gaussian form (of width $\alpha$) [2,4] for $|\omega| \gtrsim \omega_0$, to a regular Gaussian (of width $\omega_0$) for $|\omega| < \omega_0$, where $\omega_0$ is a "smearing parameter" whose significance is explained below. To obtain high-quality data, we combine small choices of $\alpha$ with an average over $N_z$ slightly shifted discretizations [3] (see [13] for more details).

*Application to Anderson model.*—We illustrate our method for the standard single-impurity Anderson model (SIAM). Its local Hamiltonian $\hat{h}_0 \equiv \sum_\sigma \epsilon_0 c_{0\sigma}^\dagger c_{0\sigma} +$
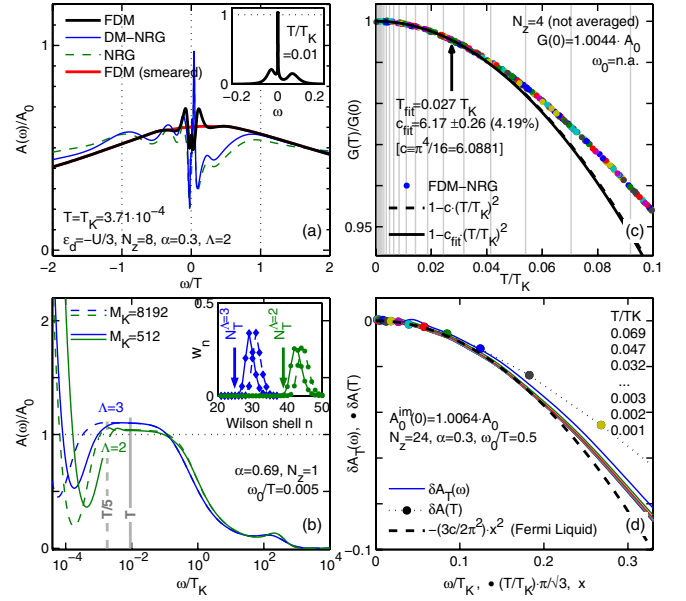


FIG. 2 (color online). FDM-NRG results for the spectral function $\mathcal{A}_T(\omega)$ of the SIAM, with $U = 0.12$, $\Gamma = 0.01$, $\epsilon_d = -U/2$ ($T_K = 2.185 \times 10^{-4}$), $\Lambda = 1.7$, and $M_K = 1024$, unless indicated otherwise. Inset of (a): FDM-NRG result for $A_T(\omega)$ with $\omega$ in units of bandwidth. For (a),(b), an unconventionally small smearing parameter was used, $\omega_0 = 0.005T$ [except for thick gray (red) curve in (a)], with $\omega_0 = 0.5T$), leading to spurious low-frequency oscillations. These illustrate the differences (a) between NRG (dashed green curve), DM-NRG [solid thin (blue) curve], and FDM-NRG (black curve) results for the regime $\omega \lesssim T$, and (b) between different choices of $M_K$ and $\Lambda$ for FDM-NRG, which yield different shapes for the weights $w_n$ [shown in inset of (b)]: larger $\Lambda$ reduces the scale $\delta_T$ at which oscillations set in, but yields less accurate values for the Kondo peak height in the regime $\delta_T \lesssim \omega \lesssim T_K$. (c),(d) Comparison of high-quality FDM-NRG data (dots, solid curves) with exact Fermi-liquid results (black dashed lines) for (c) the conductance $G(T)$ for $T \ll T_K$, and (d) for $\mathcal{A}_T^{\text{im}}(\omega)$ for $T$, $\omega \ll T_K$. In (c), $c_{\text{fit}}$ was found from a data fit to $c_{\text{fit}}(T/T_K)^2$ for $T < T_{\text{fit}}$ (arrow). In (d) we plot $\delta\mathcal{A}_T(\omega) = [A_T^{\text{im}}(\omega) - A_T^{\text{im}}(0)]/A_0^{\text{im}}(0)$ vs $\omega/T_K$ (curves) and $\delta\mathcal{A}(T) = [A_T^{\text{im}}(0)/A_0^{\text{im}}(0) - 1]$ vs $(T/T_K)\pi/\sqrt{3}$ (dots), for a set of 12 temperatures between 0.001 and $0.069T_K$ (with curves and dots having same $T$ in the same color), to illustrate the leading $\omega$ and $T$ behavior of $\mathcal{A}_T^{\text{im}}(\omega)$; the dashed black line represents the expected Fermi-liquid behavior in both cases, $-(3c/2\pi^2)x^2$ vs $x$.

$Uc_{0\uparrow}^\dagger c_{0\uparrow}c_{0\downarrow}^\dagger c_{0\downarrow}$ describes a localized state with energy $\epsilon_0$, with a Coulomb penalty $U$ for double occupancy. It is coupled to a Wilson chain $\sum_{n\sigma}\lambda_n(c_{n+1\sigma}^\dagger c_{n\sigma} + \text{H.c.})$, which generates a local level width $\Gamma$. We calculated $\mathcal{A}^<(\omega) \equiv \mathcal{A}^{c_{0\sigma}^\dagger c_{0\sigma}}(-\omega)$, $\mathcal{A}^>(\omega) \equiv \mathcal{A}^{c_{0\sigma}c_{0\sigma}^\dagger}(\omega)$ and $\mathcal{A} \equiv \mathcal{A}^> + \mathcal{A}^<$. An "improved" version $\mathcal{A}^{\text{im}}$ thereof can be obtained by calculating the impurity self-energy $\Sigma(\omega, T)$ [6,13] via FDM-NRG, which is less sensitive to smoothening details and yields more accurate results for the Kondo peak height $\mathcal{A}_{T\simeq0}(0)$ at zero temperature.

*Sum rules.*—As expected, we find FDM-NRG to be significantly more accurate at lower computational cost

than NRG or DM-NRG [8,15]. The sum rules

$$\int d\omega \, \mathcal{A}^{c_{0\sigma}^\dagger c_{0\sigma}}(\omega) = \langle c_{0\sigma}^\dagger c_{0\sigma}\rangle_T, \quad \int d\omega \, \mathcal{A}(\omega) = 1 \quad (11)$$

hold exactly to $10^{-15}$ for our discrete data, and to $10^{-4}$ after smoothing (due to numerical integration inaccuracies). Moreover, even for $M_K$ as small as 256, our results for $\mathcal{A}_{T\simeq 0}(0)$ and $\mathcal{A}_{T\simeq 0}^{\mathrm{im}}(0)$ typically agree to within 2% and 0.2%, respectively, with the Friedel sum rule, which requires $\pi\Gamma\mathcal{A}_{T=0}^{\mathrm{exact}} = \sin^2\pi\langle c_{0\sigma}^\dagger c_{0\sigma}\rangle_0$. The exact relation $\mathcal{A}^<(\omega) = f(\omega)\mathcal{A}(\omega)$ ($f$ is the Fermi function), which follows from detailed balance, is likewise satisfied well (though not rigorously so): the left-hand side of Eq. (11) typically equals $\int d\omega f(\omega)\mathcal{A}(\omega)$ to better than $10^{-4}$.

*Low-frequency data.*—Because of the underlying logarithmic discretization, all NRG-based schemes for calculating finite-temperature spectral functions inevitably produce spurious oscillations at very low frequencies $|\omega| \ll T$. The scale $\delta_T$ at which these set in can be understood as follows: the Lehmann sum in Eq. (1) is dominated by contributions from initial states $|a\rangle$ with energy $E_a \simeq T$, represented by NRG shells with $n$ near $N_T$. The characteristic energy scale of these states limits the accuracy obtainable for energy differences $E_{ba}$ to accessible final states $|b\rangle$. Thus the scale $\delta_T$ is set by those shells which contribute with largest weight $w_n$ to the density matrix.

We analyze this in more detail in Figs. 2(a) and 2(b) by purposefully choosing the smearing parameter to be unconventionally small, $\omega_0 \ll T$. The resulting spurious oscillations are usually smeared out using $\omega_0 \gtrsim \delta_T$ [Fig. 2(a), thick gray (red) curve], resulting in quantitatively accurate spectral functions only for $|\omega| \gtrsim \omega_0 \simeq \delta_T$. For conventional NRG approaches, the "single-shell" approximation $w_n = \delta_{nN_T}$ typically leads to $\delta_T \simeq T$, as can be seen in Fig. 2(a) [dashed (green) line and thin solid (blue) line]. In contrast, FDM-NRG yields a significantly reduced value of $\delta_T \simeq T/5$ [Fig. 2(a), black line, and Fig. 2(b)], since the weighting functions $w_n$ [inset of Fig. 2(b)] retain weight over several shells below $N_T$, so that lower-frequency information is included.

*Fermi-liquid relations.*—To illustrate the accuracy of our low-frequency results, we calculated $\mathcal{A}_T^{\mathrm{im}}(\omega)$ for $\omega, T \ll T_K$ for the symmetric SIAM, and made quantitative comparisons to the exact Fermi-liquid relations [14],

$$A_T(\omega) \simeq A_0\left[1 - \frac{c}{2}\left(\frac{T}{T_K}\right)^2 - \frac{3c}{2\pi^2}\left(\frac{\omega}{T_K}\right)^2\right],$$

$$G(T) \equiv \int_{-\infty}^{\infty} d\omega A(\omega, T)\left(-\frac{\partial f}{\partial \omega}\right) \simeq A_0\left[1 - c\left(\frac{T}{T_K}\right)^2\right].$$

Here $A_0 \equiv 1/\pi\Gamma$, $c \equiv \pi^4/16$, and the Kondo temperature $T_K$ is defined via the static magnetic susceptibility [4] $\chi_0|_{T=0} \equiv 1/4T_K$. Figures 2(c) and 2(d) show the FDM-NRG data [gray (colored) dots and lines] to be in remarkably good quantitative agreement with these relations (black dashed curves). The results for the "conductance"

$G(T)$, being a frequency integrated quantity obtained by summing over discrete data directly without the need for broadening, are more accurate than for $\mathcal{A}_T^{\mathrm{im}}(\omega)$, and reproduce the prefactor $c$ with an accuracy consistently within 5% (until now, accuracies of the order of 10%–30% had been customary). The smoothness of the data in Fig. 2(c), obtained using temperatures not confined to the logarithmic grid $\Lambda^{-n/2}$ [gray vertical lines in Fig. 2(b)], together with the remarkable stability with respect to different $z$ shifts illustrate the accuracy of our approach.

*Conclusions.*—Our FDM-NRG method offers a transparent framework for the calculation of spectral functions of quantum impurity models, with much improved accuracy at reduced complicational cost. Its results satisfy frequency sum rules rigorously and give excellent agreement with other consistency checks such as the Friedel sum rule, detailed balance, or Fermi-liquid relations, including the regime $\omega \lesssim T$.

*Note added.*—Just before completion of this work we learned that Peters, Pruschke, and Anders had followed up on the same idea [15].

[1] K. G. Wilson, Rev. Mod. Phys. **47**, 773 (1975); H. R. Krishnamurti, J. W. Wilkins, and K. G. Wilson, Phys. Rev. B **21**, 1003 (1980); **21** 1044 (1980).

[2] O. Sakai, Y. Shimizu, and T. Kasuya, J. Phys. Soc. Jpn. **58**, 3666 (1989).

[3] M. Yoshida, M. A. Whitaker, and L. N. Oliveira, Phys. Rev. B **41**, 9403 (1990).

[4] T. A. Costi, A. C. Hewson, and V. Zlatic, J. Phys. C **6**, 2519 (1994).

[5] T. A. Costi, Phys. Rev. B **55**, 3003 (1997).

[6] R. Bulla, A. C. Hewson, and T. Pruschke, J. Phys. C **10**, 8365 (1998).

[7] R. Bulla, T. Costi, and T. Pruschke, arXiv:cond-mat/0701105.

[8] W. Hofstetter, Phys. Rev. Lett. **85**, 1508 (2000).

[9] R. Bulla, T. A. Costi, and D. Vollhardt, Phys. Rev. B **64**, 045103 (2001).

[10] R. Bulla, N. H. Tong, and M. Vojta, Phys. Rev. Lett. **91**, 170601 (2003).

[11] F. B. Anders and A. Schiller, Phys. Rev. Lett. **95**, 196801 (2005); Phys. Rev. B **74**, 245113 (2006).

[12] F. Verstraete *et al.*, arXiv:cond-mat/0504305.

[13] See EPAPS Document No. E-PRLTAO-99-025733 for appendices which give more details. For more information on EPAPS, see http://www.aip.org/pubservs/epaps.html.

[14] A. Hewson, *The Kondo Problem to Heavy Fermions* (Cambridge University Press, New York, 1993).

[15] R. Peters, T. Pruschke, and F. B. Anders, Phys. Rev. B **74**, 245114 (2006). We recommend this paper for a more detailed comparison of the new and previous approaches.